

UKAEA-CCFE-CP(20)120

F. Schoofs, A. Cackett, J. Lim, S. M. King, A. Schiavi,
T. R. Barrett, C. Hardie

Microstructure and mechanical property mapping of CuCrZr to account for complex and non- uniform thermal history

This document is intended for publication in the open literature. It is made available on the understanding that it may not be further circulated and extracts or references may not be published prior to publication of the original when applicable, or without the consent of the UKAEA Publications Officer, Culham Science Centre, Building K1/O/83, Abingdon, Oxfordshire, OX14 3DB, UK.

Enquiries about copyright and reproduction should in the first instance be addressed to the UKAEA Publications Officer, Culham Science Centre, Building K1/O/83 Abingdon, Oxfordshire, OX14 3DB, UK. The United Kingdom Atomic Energy Authority is the copyright holder.

The contents of this document and all other UKAEA Preprints, Reports and Conference Papers are available to view online free at scientific-publications.ukaea.uk/

Microstructure and mechanical property mapping of CuCrZr to account for complex and non-uniform thermal history

F. Schoofs, A. Cackett, J. Lim, S. M. King, A. Schiavi, T. R. Barrett,
C. Hardie

Microstructure and mechanical property mapping of CuCrZr with complex and non-uniform thermal history

Frank Schoofs^a, Alexandra J. Cackett^a, Stephen M. King^b, Thomas R. Barrett^a, Christopher D. Hardie^a

^aUKAEA - United Kingdom Atomic Energy Authority, Culham Science Centre, Abingdon, United Kingdom

^bISIS - Pulsed Neutron and Muon Source, Rutherford Appleton Laboratory, Didcot OX11 0QX, United Kingdom

In this work, we present the use of small angle neutron scattering (SANS) and nanoindentation (NI) to determine the microstructural state typical of a divertor mock-up assembly, which has undergone complex heating and cooling cycles. Material property mapping is used to measure the local variation in properties throughout a component geometry, which is used to infer a variation in local stress-strain properties. It is proposed that the measurement of spatially heterogeneous material properties by these mapping techniques may provide engineers with useful insights for the design and failure analysis of components.

Keywords: CuCrZr, small angle neutron scattering, divertor

1. Introduction

CuCrZr alloys are favored in applications where a high thermal conductivity and high strength are required at elevated operating conditions, such as in heat exchange structures in a nuclear fusion reactor, e.g. ITER [1]. Precipitation hardening, with precipitate dimensions in the 1-100 nm range, is crucial to their mechanical strength during operation and therefore needs to be extremely well controlled [2]. During manufacturing and use, these components are exposed to complex, non-uniform thermal cycles, which will impact on the CuCrZr microstructure. Atom probe tomography (APT) or transmission electron microscopy (TEM) provide direct visual information of this microstructure, but only on a very small sample ($< 1 \text{ mm}^3$) [3,4]. Small angle neutron scattering (SANS), on the other hand, is able to provide a bulk measurement on millimeter-scale samples, while maintaining the sensitivity for the precipitate dimensions [5]. Here we combine SANS and nanoindentation (NI) hardness measurements to spatially map the microstructure and behavior of a single-block EU DEMO “thermal break” divertor mock-up (MUP), after fabrication [6–8].

2. Experimental methods

A single rolled tungsten block, with dimensions 12 x 23 x 30 mm and a central bore of 19 mm, containing a 1 mm cast Cu interlayer (ALMT, Japan) is brazed using an Au-Cu braze to a 15 mm diameter, 1.5 mm thick CuCrZr (Zollern GmbH & Co., 1 wt% Cr, 0.06 wt% Zr) pipe (Fig. 1a). More details of the manufacturing process will be published elsewhere [8]. The brazing cycle for the MUPs is shown in Fig. 1b – the difference between MUPs A and B is that the CuCrZr pipe in “B” has undergone this cycle twice, to improve braze flow and adhesion after removal of the segregated Zr at the surface, based on prior on-site experience with brazing this alloy.

The MUPs were cut lengthwise by wire-EDM to expose the pipe cross-section. An additional cut was made to remove the tungsten and expose the Cu interlayer. The NI sample, approximately 1 mm thick, was sliced with a third

cut from MUP A. No further sample preparation was done on the SANS samples.

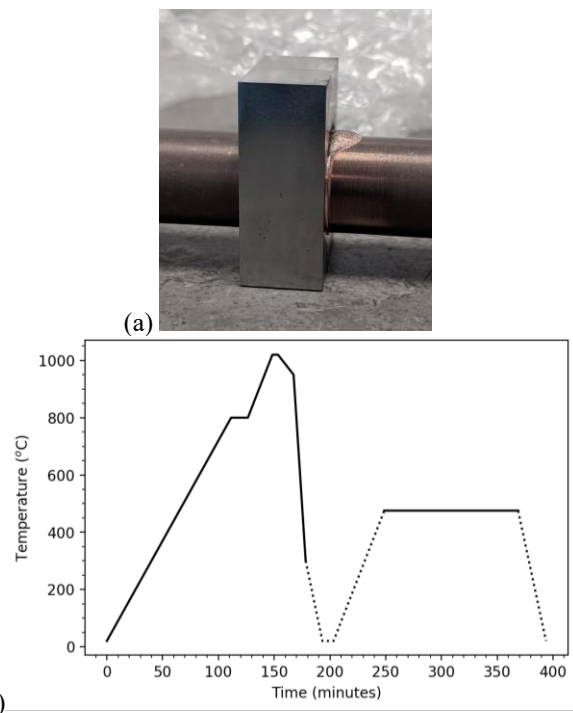


Fig. 1. (a) Photo of MUP B after brazing and before sample preparation. (b) Furnace cycle for the MUPs.

SANS was performed on the diffractometer SANS2D at the ISIS Pulsed Neutron Source [9,10]. This is a time-of-flight instrument, which means it utilizes a range of neutron wavelengths (1.75 – 16.5 Å) to simultaneously probe a very broad range of d -spacing (for the instrument configuration used, 8 – 3140 Å), and is thus ideal for the type of scoping study performed here. In the figures below, the d -spacing is expressed as the (magnitude of) the scattering vector, Q ($= 2\pi/d = 4\pi/\lambda \sin\theta$, where λ is the neutron wavelength and 2θ is the scattering angle). The beam footprint at the sample was collimated to 5 mm high and 2 mm wide. Each scattering and transmission dataset was collected for 54 and 12 minutes respectively. On each MUP, 5 measurement locations were investigated: 3 on

the pipe away from and 2 underneath the tungsten monoblock (Fig 2). Examination of the transmission data revealed prominent absorption ‘edges’ at the shorter wavelengths, a common occurrence in multi-phasic materials with crystalline regions, and so neutron wavelengths below 4.3 Å were subsequently excluded during the data reduction.

Data reduction was performed using the Mantid framework in accordance with standard procedures for SANS2D [11,12]. 2D data from the detectors were radially-averaged to 1D, using only the scattering data within sectors extending $\pm 30^\circ$ of $Q_x = 0$ to avoid artefacts, caused by a reflection of the neutrons from the edges of the pipe or the tungsten due to beam divergence. Radially-averaged data were fitted using the ODR package in SciPy [13,14] to a scattering function consisting of a combination of Porod’s law [15] and a single Lorentzian peak:

$$I = A Q^{-\alpha} + \frac{B}{1+(L*(Q-Q_{peak}))^2} + C \quad (1)$$

where α (Porod exponent) is related to the interface roughness, L (Lorentzian screening length) is related to radius of the precipitates, Q_{peak} (peak position) is related to separation of the precipitates, A and B are scaling parameters and C is the Q -independent background.

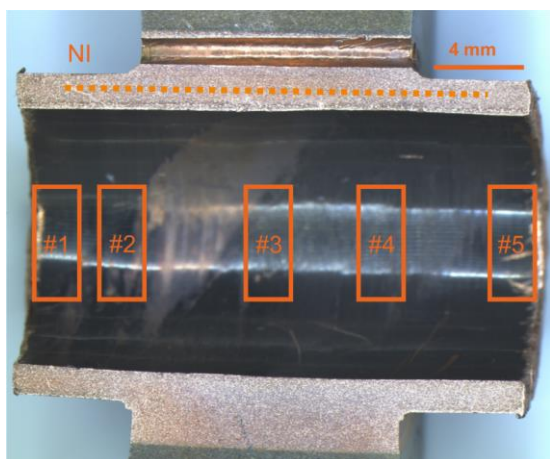


Fig. 2. Cross-section of MUP A, with the SANS (rectangles) and NI (dotted line) measurement positions indicated.

Nanoindentation testing was conducted to assess the nano-hardness along the length of the pipe as it passes through the tungsten monoblock. A slice from MUP A was polished using silicon carbide abrasive papers (up to FEPA 4000), 1 μm diamond suspension and a final chemo-mechanical polish using colloidal silica suspension (0.04 μm). A line of indents were placed with 100 μm spacing (Fig. 2). The tests were conducted with a Keysight G200 nanoindenter equipped with a Berkovich tip.

A continuous stiffness measurement (CSM) technique was used with an amplitude and frequency of 2 nm and 45 Hz respectively. The tip geometry was calibrated using a fused silica reference sample in accordance with Ref. [16]. The indents were conducted with a total depth of 2 μm and a strain rate of 0.05 s^{-1} . Measurements ($n = 13$)

were also conducted on a sample of peak aged CuCrZr for a baseline comparison (solution annealing to 980 $^\circ\text{C}$, water quenching and ageing at 480 $^\circ\text{C}$ for 2 hours) [1].

3. Results and discussion

The radially-averaged 1D data (Fig. 3) all show a similar Q -dependence: a power law decay at low- Q followed by an inflection leading to a broad peak at higher- Q . The Porod exponent, from fitting with equation (1), hardly fluctuates over the length of the pipe (Fig. 4a). The value is also close to the ‘‘ideal’’ of 4, suggesting the scattering centers (precipitates) have a good coherency with the matrix. Interestingly, there appears to be a subtle variation in the precipitate size (Fig. 4b), with a slight increase in size being observed underneath the tungsten monoblock. The diameter of the precipitates is in line with TEM analysis of optimum aged material, with slight overaging under the tungsten block [17]. This would be consistent with a subtly different thermal response of the CuCrZr due to the locally different thermal mass.

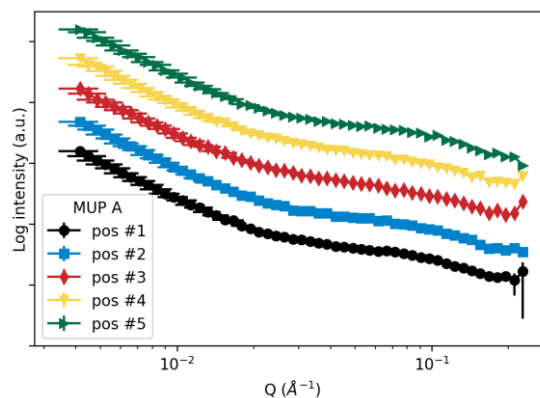


Fig. 3. Comparison of SANS curves at different positions in MUP A. The curves are vertically offset for clarity.

The precipitate separation under the W block was difficult to fit reliably, presumably due to additional scattering. In the CuCrZr pipe away from the W, the average distance is approximately 32 \pm 4 nm in MUP A and 27 \pm 4 nm in MUP B, which corresponds to an approximate number density of $(0.80 \pm 0.27) \times 10^{22} \text{ m}^{-3}$ and $(1.40 \pm 0.75) \times 10^{22} \text{ m}^{-3}$ in MUP A and B respectively. Comparing to the TEM-based values obtained for CuCrZr annealed at different temperatures, this suggests the MUP pipes are comparable to slightly overaged material [17].

Fig. 5 shows the average modulus and hardness results from nanoindentation for positions along the pipe. The elastic modulus is 137 GPa (3 s.f.) \pm 5 GPa standard deviation; this corresponds well to the elastic modulus of the peak aged material of 135 GPa \pm 3.4 GPa standard deviation (called baseline value in the figure) which has been measured using identical techniques. The average hardness of the pipe material was 1.71 GPa \pm 0.11 GPa which also corresponds well to the average hardness for the baseline material of 1.75 GPa \pm 0.06 GPa. Indentation tests were not placed in the region 13-14 mm to avoid sample damage and debris in that area, therefore there is a gap in the data at this point. Any apparent weak trend

within the scatter in hardness results corresponds to a proportional change in the measured modulus and is therefore likely the cause of local variation in compliance within the load train rather than a genuine variation in mechanical properties of the material.

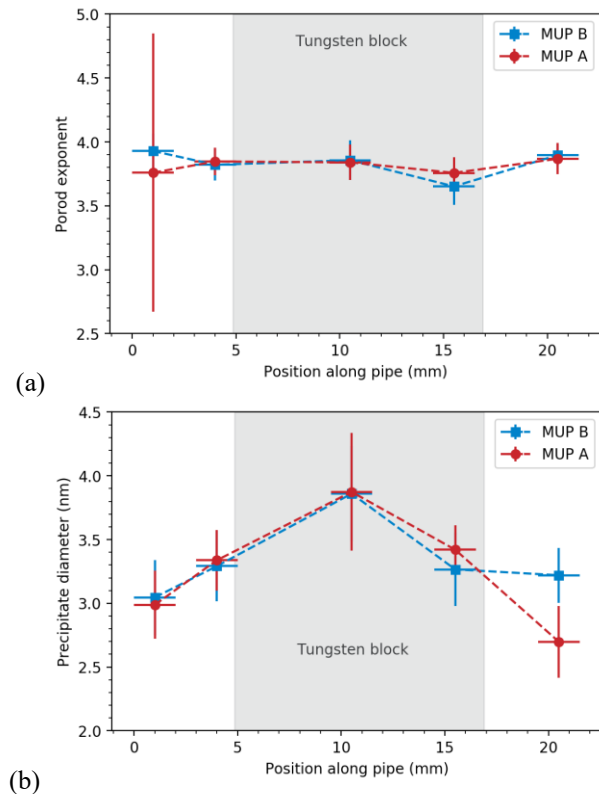


Fig. 4. Variation of fitted (a) Porod exponent and (b) precipitate diameter across the length of the pipe for both MUPs.

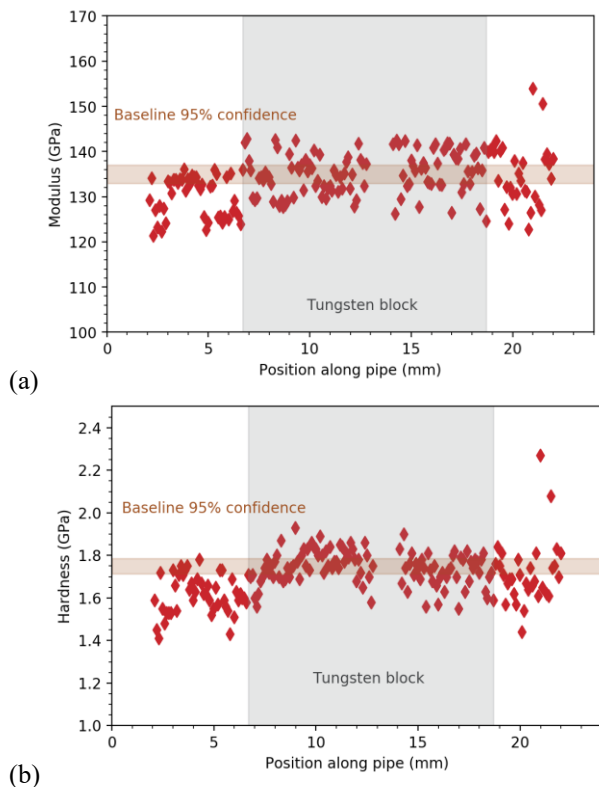


Fig. 5. Average values of NI (a) elastic modulus and (b) hardness for data produced over indentation depth of 1 to 2 μm . A 95% confidence interval around the baseline is indicated by an orange box.

4. Conclusions

In summary, we have demonstrated that SANS can be used to resolve the state of CuCrZr precipitates at a millimeter scale on divertor components, with minimal sample preparation required. The manufacturing method for the thermal break EU divertor concept studied here, namely brazing the solution annealed CuCrZr pipe, followed by a gas quench and an ageing treatment, is demonstrated to give near-optimal mechanical properties, with only subtle variations underneath the tungsten monoblock, suggesting slight over-ageing, as detected by SANS. The NI results are in line with the baseline, optimum aged material. Further work could include other manufacturing methods, as well as full divertor mock-ups that have been exposed to cyclic high heat fluxes.

Acknowledgments

This project was funded by the RCUK Energy Programme (grant number EP/I501045) and the EMPIR Programme (14IND03), co-financed by the Participating States and from the European Union's Horizon 2020 research and innovation programme. Equipment at the Materials Research Facility at UKAEA was used; the MRF is funded by the UK National Nuclear User Facility (EP/I037644/1) and Henry Royce Institute (EP/P021727/1). We would also like to thank the Science & Technology Facilities Council for the provision of neutron beamtime at ISIS (Experiment RB1790202). To obtain further information on the data and models underlying this paper please contact PublicationsManager@ukaea.uk.

References

- [1] G.M. Kalinin, A.D. Ivanov, A.N. Obushev, B.S. Rodchenkov, M.E. Rodin, Y.S. Strebkov, Ageing effect on the properties of CuCrZr alloy used for the ITER HHF components, *J. Nucl. Mater.* 367–370 (2007) 920–924. doi:10.1016/j.jnucmat.2007.03.256.
- [2] A.D. Ivanov, A.K. Nikolaev, G.M. Kalinin, M.E. Rodin, Effect of heat treatments on the properties of CuCrZr alloys, *J. Nucl. Mater.* 307–311 (2002) 673–676.
- [3] A. Chbihi, X. Sauvage, D. Blavette, Atomic scale investigation of Cr precipitation in copper, *Acta Mater.* 60 (2012) 4575–4585. doi:10.1016/j.actamat.2012.01.038.
- [4] M. Hatakeyama, T. Toyama, Y. Nagai, M. Hasegawa, M. Eldrup, B.N. Singh, Nanostructural Evolution of Cr-rich Precipitates in a Cu-Cr-Zr Alloy During Heat Treatment Studied by 3 Dimensional Atom Probe, *Mater. Trans.* 49 (2008) 518–521. doi:10.2320/matertrans.MBW200736.
- [5] Y.B. Melnichenko, *Small-Angle Scattering from Confined and Interfacial Fluids*, Springer International Publishing, 2016.
- [6] T.R. Barrett, S.C. McIntosh, M. Fursdon, D. Hancock,

- W. Timmis, M. Coleman, M. Rieth, J. Reiser, Enhancing the DEMO divertor target by interlayer engineering, *Fusion Eng. Des.* 98–99 (2015) 1216–1220. doi:10.1016/j.fusengdes.2015.03.031.
- [7] J.H. You, E. Visca, T. Barrett, B. Böswirth, F. Crescenzi, F. Domptail, M. Fursdon, F. Gallay, B.E. Ghidersa, H. Greuner, M. Li, A. V. Müller, J. Reiser, M. Richou, S. Roccella, C. Vorpahl, European divertor target concepts for DEMO: Design rationales and high heat flux performance, *Nucl. Mater. Energy.* 16 (2018) 1–11. doi:10.1016/j.nme.2018.05.012.
- [8] T.R. Barrett, M. Fursdon, F. Domptail, A. Lukenskas, F. Schoofs, H. Greuner, S. Roccella, E. Visca, F. Gallay, M. Richou, J.H. You, High heat flux test results for a thermal break DEMO divertor target and subsequent design and manufacture development, 2018.
- [9] SANS2D, (n.d.). <https://www.isis.stfc.ac.uk/Pages/sans2d.aspx>.
- [10] R.K. Heenan, S.E. Rogers, D. Turner, A.E. Terry, J. Treadgold, S.M. King, Small Angle Neutron Scattering Using Sans2d, *Neutron News.* 22 (2011) 19–21.
- [11] Mantid Project, Mantid: Manipulation and Analysis Toolkit for Instrument Data, (2013). doi:<http://dx.doi.org/10.5286/SOFTWARE/MANTID>.
- [12] O. Arnold, J.C. Bilheux, J.M. Borreguero, A. Buts, S.I. Campbell, L. Chapon, M. Doucet, N. Draper, R. Ferraz Leal, M.A. Gigg, V.E. Lynch, A. Markvardsen, D.J. Mikkelsen, R.L. Mikkelsen, R. Miller, K. Palmen, P. Parker, G. Passos, T.G. Perring, P.F. Peterson, S. Ren, M.A. Reuter, A.T. Savici, J.W. Taylor, R.J. Taylor, R. Tolchenov, W. Zhou, J. Zikovsky, Mantid—Data analysis and visualization package for neutron scattering and μ SR experiments, *Nucl. Instruments Methods Phys. Res. Sect. A Accel. Spectrometers, Detect. Assoc. Equip.* 764 (2014) 156–166. doi:<https://doi.org/10.1016/j.nima.2014.07.029>.
- [13] E. Jones, T. Oliphant, P. Peterson, others, SciPy: Open Source Scientific Tools for Python, (n.d.).
- [14] P.T. Boggs, J.E. Rogers, Orthogonal Distance Regression, in: *Stat. Anal. Meas. Error Model. Appl. Proc. AMS-IMS-SIAM Jt. Summer Res. Conf.*, 1989.
- [15] P.W. Schmidt, Small-angle scattering studies of disordered, porous and fractal systems, *J. Appl. Crystallogr.* 24 (1991) 414–435. doi:10.1107/S0021889891003400.
- [16] W.C. Oliver, G.M. Pharr, An improved technique for determining hardness and elastic modulus using load and displacement sensing indentation experiments, *J. Mater. Res.* 7 (1992) 1564. doi:10.1080/14786444908521733.
- [17] A.J. Cackett, J.J.H. Lim, P. Klups, A.J. Bushby, C.D. Hardie, Using spherical indentation to measure the strength of copper-chromium-zirconium, *J. Nucl. Mater.* (2018). doi:10.1016/j.jnucmat.2018.04.012.